$SU(4)$ string tensions from the fat-center-vortices model

S. Deldar[a], S. Rafibakhsh[b]

Department of Physics, University of Tehran, P.O. Box 14395/547, Tehran 1439955961, Iran

Abstract. The thick- or fat-center-vortices model has been applied to a calculation of the potentials between static sources of various $SU(4)$ representations. For intermediate distances, a linear potential is obtained. For this region the string tensions agree qualitatively with both flux tube counting and Casimir scaling, even though for some representations it favors flux tube counting more. In addition, our results confirm the existence of two different string tensions for non-zero 4-ality representations at large distances. In this area, zero 4-ality representations are screened. In our computations, we have used only the first non-trivial vortex of $SU(4)$.

PACS. 11.15 Ha, 12.38 Aw, 2.39 Pn

1 Introduction

It has almost been proved that QCD is the true theory of the strong interactions. For the high energy regime (asymptotically free region), the perturbative formulation shows impressive agreement between theory and experiment. Lots of efforts have been made for the low energy region where a non-perturbative formulation is required and people are interested to see confinement which is one of the main features of QCD. It is shown by many numerical measurements in $SU(2)$, $SU(3)$ and $SU(4)$ lattice gauge theory [1,2] that at intermediate distances a linear potential between the quarks for the fundamental and higher representations exists and the string tension is representation dependent and roughly proportional to the eigenvalue of the quadratic Casimir operator of the representation. This proportionality of the potential to the Casimir operator is called "Casimir scaling". On the other hand some physicists argue for flux counting and describe the linear behavior of the potentials at intermediate distances based on this idea [3,4] which claims that the string tension at intermediate distances is proportional to the number of fundamental flux tubes embedded into the representation. Flux tube counting is supposed to coincide with Casimir scaling in the large N limit.

Besides numerical calculations, people have been trying to introduce phenomenological models to explain confinement in QCD. One of these models is the center-vortex theory introduced in the late 1970's [5]. This model has been developed by Faber et al. [6] to the thick-center-vortices model to study the linearity of the potential for

higher representations and has been tested for quarks in $SU(2)$. In this paper, we apply the thick- or fat-center-vortices model to the sources of $SU(4)$. The representations 4 (fundamental), 6, 10, 15 (adjoint), 20 and 35 of $SU(4)$ are studied. Each representation is shown by (n, m), where n and m are the number of original quarks and antiquarks (in the fundamental representation) anticipated in producing the representation. Then since a quark in representation 10, for example, is constructed from two quarks and no antiquark:

$$4 \otimes 4 = 10 \oplus 6. \tag{1}$$

10 is shown by (2,0). Other representations are shown as follows: 4: (1,0), 6: (2,0), 15: (1,1), 20: (3,0) and 35: (4,0). Our results from the thick-center-vortices model indicate that quarks in all representations of $SU(4)$ are confined at intermediate distances. For large distances their behavior is based on the 4-ality. Representations with zero 4-ality are screened and other potentials will be parallel to the potential of either the fundamental representation or representation 6. I recall that for the $SU(4)$ gauge group, at large distances two different string tensions are expected. The general behavior of quarks in $SU(4)$ is in agreement with previous works by Faber et al. [6] and Deldar [7] for $SU(2)$ and $SU(3)$, respectively. At large distances the potential between two sources is large enough and a pair of adjoint sources releases from the vacuum. Therefore based on the N-ality of the representation, we expect to see screening or change of the slope of the potential to the slope of the potential in the fundamental representation. This behavior has been observed for $SU(2)$, for example, and reported in [6], where at large distances the screening occurs for the adjoint representation and the slope of the

[a] e-mail: sdeldar@khayam.ut.ac.ir
[b] e-mail: shrafi@phymail.ut.ac.ir

potential for $j = 3/2$ becomes equal to that of the fundamental representation. For $SU(3)$, the representations 3, 6, 8, 10, 15s, 15a and 27 are studied. Results obtained for $SU(2)$ and $SU(3)$ at intermediate distances show a qualitative agreement with Casimir scaling. In this paper, we show that for $SU(4)$ quarks, one can get two asymptotic string tensions by choosing the parameters of the model appropriately. As studied for $SU(3)$ [7], the approximate Casimir scaling would be obtained, if one chooses a physical profile for the vortex. For $SU(4)$, we use one of the pretested profiles which seems physical and has worked well for $SU(2)$ and $SU(3)$. There are two different vortices for $SU(4)$. For simplicity in the computations, we use only one of them and show that one can still get linear potentials for all representations at intermediate distances. Comparing the results of the $SU(3)$ and $SU(4)$ gauge groups, we show that even though the potentials are proportional to Casimir scaling, a tendency to flux tube counting is also observed.

In addition, we take a closer look at the $SU(3)$ lattice data for the inter-quark potentials at intermediate distances. We discuss the possibility of string tensions to be proportional to Casimir operators as well as the number of fundamental fluxes.

In Sect. 2, we review very briefly the thick-center-vortices model, and then the results of applying this model to $SU(4)$ are given in Sect. 3.

2 Calculation of the potentials in $SU(4)$ by the thick-center-vortices model

Vortex condensation theory [5] claims that the QCD vacuum is filled with closed magnetic vortices that have the topology of tubes or surfaces of finite thickness which carry magnetic flux quantized in the element of the center of the gauge group. In order for the vortex to have a finite energy per unit length, the gauge potential at large transverse distances must be a pure gauge. However, the gauge transformation which produces that potential is non-trivial. It is discontinuous by an element of the gauge center. The non-trivial nature of the gauge transformation forces the vortex core to have non-zero energy and makes the vortex topologically stable. A center vortex linked to a Wilson loop, in the fundamental representation of $SU(N)$, has the effect of multiplying the Wilson loop by an element of the gauge group center, i.e.

$$W(C) \rightarrow \exp^{\frac{2\pi i n}{N}} W(C), \qquad n = 1, 2, ..., N - 1. \quad (2)$$

The vortex theory states that the area law for the Wilson loop is due to the quantum fluctuation in the number of center vortices linking the loop. The QCD vacuum does not tolerate a linear potential between adjoint quarks over an infinite range. Since adjoint color charges are screened by gluons, the force between these sources drops to zero and this is exactly what happens in the center vortex theory. However for intermediate distances, a linear regime is reported by lattice calculations for quarks of higher representations. The string tension for quarks

of a higher representation is obtained if the vortex thickness is quite large: on the order of the typical diameters of low-lying hadrons. These vortices are called thick-center-vortices [6]. The thick-center-vortices model uses two basic assumptions to get confinement for sources of higher representations. The first assumption describes that the effect of creating a center vortex piercing the minimal area of a Wilson loop may be represented by the insertion of a unitary matrix at some point along the loop. This matrix depends on the flux distribution of the vortex and the generators of the group in each representation. The second assumption says that the probabilities f that loops in the minimal area are pierced by vortices and also the random group orientations associated with the gauge group elements in each representation are uncorrelated and should be averaged. Then the average Wilson loop is

$$\langle W(C) \rangle = \prod_x \left\{ 1 - \sum_{n=1}^{N-1} f_n (1 - \mathrm{Re}\,\mathcal{G}_r[\boldsymbol{\alpha}_C^n(x)]) \right\}, \quad (3)$$

x is the location of the center of the vortex and C indicates the Wilson loop and $\mathcal{G}_r$ is defined as

$$\mathcal{G}_r[\boldsymbol{\alpha}] = \frac{1}{d_r} \mathrm{Tr} \exp[i\boldsymbol{\alpha}.\boldsymbol{H}], \quad (4)$$

where d_r is the dimension of the representation and $\{H_i, i = 1, 2, ..., N - 1\}$ are generators spanning the Cartan subalgebra. f is the probability that any given unit is pierced by a vortex. The parameter $\alpha_C(x)$ describes the vortex flux distribution and depends on the vortex location; in other words, it depends on what fraction of the vortex core is enclosed by the Wilson loop. Therefore, it depends on the shape of the loop and the position of the center of the vortex in the plane of loop C relative to the perimeter.

On the other hand, the potential may be found by measuring the Wilson loop and looking for the area law fall-off at large T:

$$W(R, t) \simeq \exp^{-V(R)T}, \quad (5)$$

where R is the spatial separation of the quarks, T is the propagation time, and $V(R)$ is the gauge field energy associated with the static quark–antiquark source. For the thick-center-vortices model, T is assumed to be fixed and very huge compared to R. Therefore the loop C is just characterized by the width R. Thus from (3) and (5) the inter-quark potential induced by the vortices is

$$V(R) = \sum_x \ln \left\{ 1 - \sum_{n=1}^{N-1} f_n (1 - \mathrm{Re}\,\mathcal{G}_r[\boldsymbol{\alpha}_C^n(x)]) \right\}. \quad (6)$$

$V(R)$ depends on $\alpha_C(x)$ (its shape and size) which is determined by the fraction of the vortex flux that is enclosed by the Wilson loop.

Vortices of type n and $N - n$ are the same, except that the magnetic fluxes are in opposite directions:

$$f_n = f_{N-n} \quad \text{and} \quad \mathcal{G}_r[\boldsymbol{\alpha}_C^n(x)] = \mathcal{G}_r^{\star}[\boldsymbol{\alpha}_C^{N-n}(x)]. \quad (7)$$

There are three types of vortices in $SU(4)$. Because of (7), $f_1 = f_3$, and $\text{Re}\mathcal{G}_r[\boldsymbol{\alpha}_C^1(x)] = \text{Re}\mathcal{G}_r[\boldsymbol{\alpha}_C^3(x)]$ and therefore

$$\langle W(C) \rangle = \prod_x \left\{ 1 - 2f_1(1 - \text{Re}\mathcal{G}_r[\boldsymbol{\alpha}_C^1(x)]) \right.$$
$$\left. - f_2\left(1 - \text{Re}\mathcal{G}_r\left[\boldsymbol{\alpha}_C^2(x)\right]\right) \right\}. \quad (8)$$

To make the computation simpler, we assume $f_2 = 0$. This means that mainly the first non-trivial center element contributes and in fact it agrees with other studies of vortices [8]. $\mathcal{G}_r$ for vortex number 1 is

$$\mathcal{G}_r[\boldsymbol{\alpha}] = \frac{1}{d_r}\text{Tr}\exp[\text{i}(\alpha_1^1 H_1 + \alpha_2^1 H_2 + \alpha_3^1 H_3)]. \quad (9)$$

The upper index of α shows the vortex profile for vortex number 1 which is associated with f_1. If one wants to include vortex number 2 in the computations, one may choose another vortex profile with upper index 2. Vortex number 2 is associated with f_2. The diagonal elements of the Cartan subalgebra in $SU(4)$ are

$$H_1 : \frac{1}{2\sqrt{6}}(1, 1, 1, -3),$$
$$H_2 : \frac{1}{2\sqrt{3}}(1, 1, -2, 0),$$
$$H_3 : \frac{1}{2}(1, -1, 0, 0). \quad (10)$$

Only H_1 is a $4*4$ matrix with all diagonal elements non-zero, and the other two come from the $SU(2)$ and $SU(3)$ gauge groups. Because of this fact, one may use only H_1 and α_1^1 in the calculations and thus (9) reduces to

$$\mathcal{G}_r[\boldsymbol{\alpha}] = \frac{1}{d_r}\text{Tr}\exp[\text{i}\alpha_1^1 H_1]. \quad (11)$$

The real part of the trace of $\mathcal{G}_r[\boldsymbol{\alpha}]$ in (11), with appropriate normalization factor of α, contains the real part of the trace of (9). So again, for simplicity we use (11). Calculating the normalization factor for α's is discussed later.

The appropriate flux distribution, $\alpha(x)$, can be chosen such that a well behaved potential is obtained. This means that with a good choice, one can see the linear term of the potential for all representations. In general any physical axially symmetric density distribution for the vortex leads to potentials which are acceptable in QCD. A variety of different fluxes is introduced in [7]. Here we choose $\alpha_c(x)$ to be

$$\alpha_R(x) = \left(\frac{\sqrt{6}\pi}{2}\right)\left[1 - \tanh\left(ay(x) + \frac{b}{R}\right)\right]; \quad (12)$$

a, b and f are constants and are free parameters of the model. They must be chosen such that a linear potential at intermediate distances as well as proportionality with Casimir scaling are observed. In this paper $a = 0.05$, $b = 4$, $f_1 = 0.1$ and

$$y(x) = \begin{cases} x - R & \text{for } |R - x| \le |x|, \\ -x & \text{for } |R - x| > |x|, \end{cases} \quad (13)$$
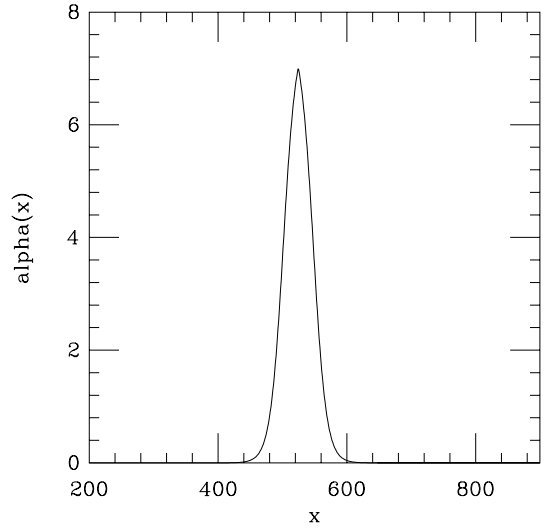
Fig. 1. Flux distribution of (12). For this plot $R = 50$ and the Wilson loop may entirely overlap the vortex core

The normalization factor for α is obtained based on the assumptions of the model. Equation (2) shows that each time that a vortex links to a fundamental Wilson loop, the loop is multiplied by the factor $\exp\frac{2\pi\text{i}n}{N}$. Since we are using only one vortex and $N = 4$, we have

$$W(C) \to \exp\frac{\pi\text{i}}{2} W(C). \quad (14)$$

Thus, based on the thick-center-vortices model, for higher representations, every time that the minimal surface is pierced by a center vortex, a center element $\exp\left(\frac{\pi\text{i}}{2}\right)$ should be inserted somewhere along the loop:

$$W(C) = \text{Tr}[UU...U] \to \text{Tr}\left[UU...\exp\left[\frac{\pi\text{i}}{2}\right]...U\right]. \quad (15)$$

Using this fact and the point that we have used only one vortex and only H_1 in our computations, the normalization factor is obtained from $\exp\frac{\pi\text{i}}{2} = \exp^{\text{i}\alpha H_1}$ which happens if the vortex core is entirely contained within the Wilson loop. Therefore α should satisfy the following conditions.
(1) Vortices which pierce the plane far outside the loop do not affect the loop. In other words, for fixed R, as $x \to \infty$, $\alpha \to 0$.
(2) If the vortex core is entirely contained within the loop, then $\alpha = \sqrt{6}\pi$.
(3) As $R \to 0$ then $\alpha \to 0$.
    Equation (12) with its normalization factor satisfies the above conditions. Changing the parameters a and b by any factor F and setting $a \to \frac{a}{F}$ and $b \to bF$ only changes the scale of the potential and the physics remains the same. However not any arbitrary value for a and b leads to a linear potential.
    Figure 1 shows this flux distribution versus x, the location of the center of the vortex. For this plot $R = 50$. Thus the size of the loop is such that the vortex may overlap completely the Wilson loop. Another example of
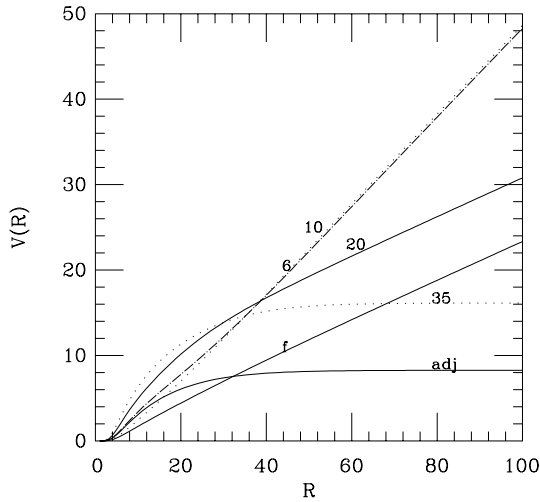
Fig. 2. Static sources potential for the range of $R \in [1, 100]$. At intermediate distances, potentials are linear. At large distances, representations 15 (adjoint) and 35 are screened; representation 20 gets the same slope as the fundamental representation and representation 10 is parallel to representation 6

Table 1. This table shows Casimir numbers ratios, number of flux tubes and string tensions ratios for the $SU(4)$ gauge group. A qualitative agreement of string tensions with both Casimir scaling and flux tube counting is observed

Repn.	4 (fund.)	6	15a	10	20	35
(n, m)	$(1, 0)$	$(2, 0)$	$(1, 1)$	$(2, 0)$	$(3, 0)$	$(4, 0)$
c_r/c_f	1	1.33	2.13	2.4	4.2	6.4
fund. fluxes	1	2	2	2	3	4
k_r/k_f	1	1.51	1.56	1.76	2.31	2.66

Table 2. The same as Table 1 but for the $SU(3)$ gauge group

Repn.	3 (fund.)	8	6	15a	10	27	15s
(n, m)	$(1, 0)$	$(1, 1)$	$(2, 0)$	$(2, 1)$	$(3, 0)$	$(2, 2)$	$(4, 0)$
c_r/c_f	1	2.25	2.5	4	4.5	6.	7
fund. fluxes	1	2	2	3	3	4	4
k_r/k_f	1	2.02	2.21	3.1	3.4	3.8	5.6

a physical flux distribution is the one which is zero everywhere except on the boundary of the vortex [7]. A density proportional to a delta function which is zero everywhere except at the two points where the vortex first enters and exits the Wilson loop is among the non-axially symmetric distributions. Using this flux, one loses Casimir scaling proportionality.

3 Results and discussion

Figure 2 shows the potentials for various representations versus R in the range $R \in [1, 100]$. For all representations, there is a region where the potentials are linear (about $R \in [5, 15]$). In general, at large distances, screening for 15 (adjoint) and 35 should occur. 4-ality which is (n, m) mod 4, is zero for representations 15: $(1, 1)$ and 35: $(4, 0)$. Screening is expected for zero 4-ality representations. In fact, at large distances, the potential between two sources is large enough to create a pair of quarks in the adjoint representation (15) from the vacuum. Then the original static sources combine with the 15s and for zero 4-ality representations a 15 component is created and the potential will be screened. For non-zero 4-ality representations, two possible scenarios may occur: for example, for representation 20, a fundamental component will be created and therefore the slope of the potential changes to that of the fundamental representation; on the other hand, for 6 and 10 dimensional diquark representations, a quark in representation 6 is created and the slope of the potential in representation 10 changes to the slope of the potential in the representation 6. We have

$$15 \otimes 6 = 64 \oplus 10 \oplus \bar{1}0 \oplus 6, \tag{16}$$
$$15 \otimes 10 = 70 \oplus 64 \oplus \bar{1}0 \oplus 6. \tag{17}$$

This is why there are two different string tensions, one for the 4 and another for the 6 dimensional representation. For the $SU(N)$ gauge group with $N > 3$, there is more than one asymptotic string tension. In $SU(4)$, potentials of the 6 and 10 dimensional representations do not parallel the fundamental representation potential and the slope of the potential of representation 10 changes to that of representation 6 [10]. Using only vortex number 1 in our calculations, $f_2 = 0$, we have gotten two different string tensions for the $SU(4)$ sources.

Figure 3 plots the ratios of the potential of each representation to that of the fundamental one. Although these ratios start up roughly at the ratios of the corresponding Casimirs, which are 1.3, 2.4, 2.13, 4.2 and 6.4 for the representations 6, 10, 15, 20 and 35, respectively, but in the most linear part of the potential (Fig. 4), the ratios of some representations are closer to the flux tube counting. Table 1 shows the representations we have studied with the number of original quarks and antiquarks, (n, m), anticipated in each representation. In the third row, the ratio of Casimir number of each representation to that of the fundamental one is indicated. The number of fundamental fluxes existing in each representation is shown in the fourth row. The last row indicates the ratio of the string tension of each representation to the fundamental one, calculated from this work. These string tensions are obtained from the range of $R \in [5, 12]$ which is the most linear part of the potentials in our calculations. The agreement with both Casimir scaling and flux counting is qualitative, but it favors flux tube counting more. Comparing Tables 1 and 2, one can see that the tendency to the flux tube counting increases by increasing the number of gauge groups, especially for the representations 35 of $SU(4)$ and 15s of $SU(3)$.
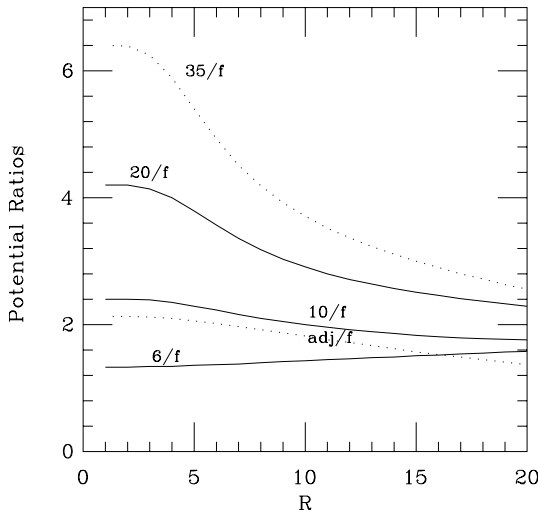
Fig. 3. Potential ratio of each representation to the fundamental representation. These ratios start up roughly at the ratios of the corresponding Casimirs, which are 1.3, 2.4, 2.13, 4.2 and 6.4 for representations 6, 10, 15, 20 and 35, respectively, but in the most linear part of the potential (Fig. 4), the ratios are also in agreement with the flux tube counting especially for the higher representations. The slope of the potentials will become constant after the confinement regime is finished. It happens at about $R = 30$ with the given parameters (a, b, f) we used in the model
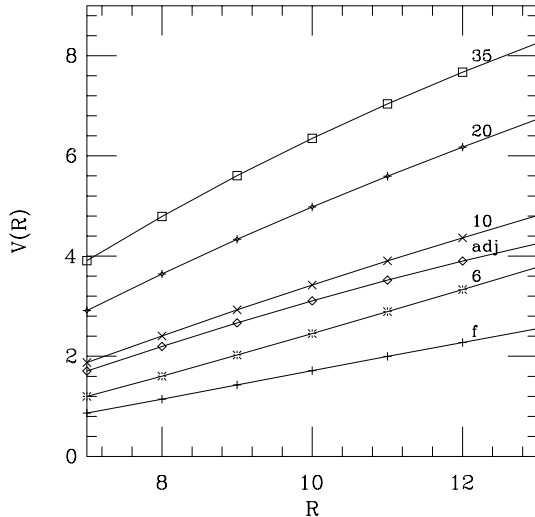
Fig. 4. The most linear part of the potentials. The slope of each potential is obtained for the range $R \in [7, 12]$. They are .282, .427, .439, 498, .652 and .752 for representations fundamental, 6, adjoint, 10, 20 and 35, respectively. The ratios of string tensions (slopes of the linear part of potentials) are reported in Table 1

Looking closer at Fig. 3, it seems that there are four regions for the potentials. For the first area, basically for $R < 5$, the potentials are proportional to Casimir scaling; especially for very small R. The potential ratios start out at the ratios of Casimirs which are larger than the number of fundamental fluxes, but they get close to the number of fluxes embedded in each representation at about $R = 10$
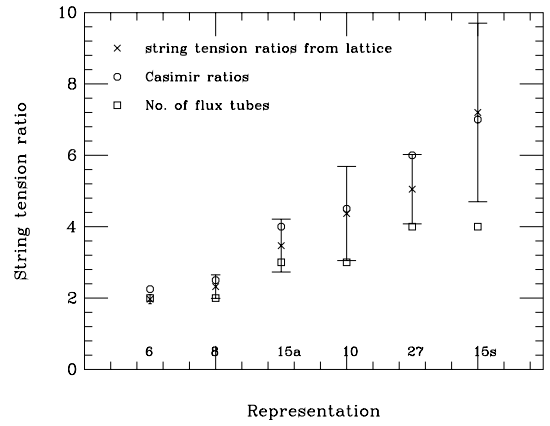
Fig. 5. Ratios of string tensions of $SU(3)$ quarks of different representations to the string tension of quarks in the fundamental representation are plotted. Considering the lattice data errors, good agreement with both Casimir scaling and flux tube counting is observed

for the representations 35, 20 and 10 and at about $R = 20$ for representations 15 (adjoint) and 6. Based on the assumptions of the thick-center-vortices model, vortices are uncorrelated and also the orientation of the "vortex insertion" in color space is chosen at random. Thus, it might be possible that these assumptions lead effectively to the interaction of flux tubes. Then one may explain the behavior of the potentials at different distances by the interaction between fundamental strings as follows: When the distance between sources is very small, the fundamental fluxes overlap and the string tension is larger than the number of fluxes times the fundamental string tension. This is because of the repulsion between the fluxes [4]. This may explain the behavior of the potential for distances less than 5 in Fig. 3. On the other hand as the distance increases, the fluxes tend to attract each other and therefore a negative energy is added to the binding energy of fluxes and this makes the string tension smaller (for $10 < R < 20$) [4,9]. In general if there is no interaction between the fluxes, the string tension of the representation must be $K\sigma_f$ where K is the number of fundamental fluxes and σ_f is the fundamental string tension. Screening or change of the slope of the potentials starts from about $R = 30$.

Casimir scaling obtained from $SU(3)$ lattice calculations by Bali [3] has been verified for distances less than 1 fm and the ratios are reported to be bigger than the number of fluxes. It seems that the thermal distance between strings in the lattice results is not large enough and an overlap between the strings leads to a repulsion force and therefore increasing of the string tension. This coincides with the $R < 5$ of Fig. 2. It should be noticed that the scales of R and $V(R)$ are arbitrary (adjustable) in the thick-center-vortices model. On the other hand, the results reported by Deldar [7] are obtained for larger distances (up to 2.5 fm). Figure 5 is plotted based on the data of [7]. Cross signs show the ratios of the string tensions of $SU(3)$ sources of various representations to that of the fundamental representation. Circles indicate Casimir

ratios, and diamonds show the number of fundamental strings in each representation. As claimed by the lattice people, the ratios of the string tensions are proportional to the Casimir operators. On the other hand, the plot shows that there is a rough agreement with the number of fundamental tubes as well. One may conclude that the errors of the lattice data are still too large to discriminate between the two hypotheses, Casimir scaling and flux counting.

4 Conclusion

Using thick-center-vortices model, we have shown that for all representations at intermediate distances there is a region where quarks are confined and the potentials are linear. For this linear regime, our results show evidence of proportionality of the string tensions with both Casimir scaling and flux counting even though the agreement is slightly better for the flux tube counting. At large distances, zero 4-ality representations (15, 35) are screened, the potential of the representation 20 has become parallel to that of the fundamental representation and the potentials of the diquark representations (6 and 10) get the same slope. In our computations, we have used only the first non-trivial vortex of $SU(4)$. Although we have not used vortex number 2 in our calculations, our results at intermediate distances agree with lattice results and the potentials are linear and qualitatively in agreement with Casimir scaling at intermediate distances.

We are doing new computations with f_2 not necessarily zero and study the effect of vortex number 2 and also the different core sizes of the vortices in the linear region of the potential. Especially, we are interested in studying the effect of different parameters of the model on removing the concavity of the potentials which has been observed for $SU(2)$ and $SU(3)$ sources, as well.

References

1. C. Bernard, Phys. Lett. B **108**, 431 (1982); Nucl. Phys. B **219**, 341 (1983); J. Ambjørn, P. Olesen, C. Peterson, Nucl. Phys. B **240**, 189 (1984); C. Michael, Nucl. Phys. B **259**, 58 (1985); G. Poulis, H. Trottier, Phys. Lett. B **400**, 358 (1997); S. Ohta, M. Wingate, Nucl. Phys. **83** (Proc. Suppl.), 381 (2000)
2. G. Bali, Phys. Rev. D **62**, 114503 (2000); S. Deldar, Phys. Rev. D **62**, 034509 (2000)
3. C. Michael, Adiabatic surfaces from the lattice excited gluonic potentials, hep-ph/9809211; G.S. Bali, Phys. Rept. **343**, 1 (2001)
4. A. Armoni, M. Shifman, Nucl. Phys. B **671**, 67 (2003)
5. G 't Hooft, Nucl. Phys. B **153**, 141 (1979); J.M. Cornwall, Nucl. Phys. B **153**, 392 (1979); G. Mack, V.B. Petkova, Ann. Phys. (NY) **123**, 442 (1979); **125**, 117 (1980); Z. Phys. C **12**, 177 (1982); H.B. Nielson, P. Olesen, Nucl. Phys. B **160**, 380 (1979); J. Ambjørn, P. Olesen, Nucl. Phys. B **170**, 265 (1980); B **170**, 60 (1980); L.G. Yaffe, Phys. Rev. D **21**, 1574 (1980)
6. M. Faber, J. Greensite, S. Olejnik, Phys. Rev. D **57**, 2603 (1998)
7. S. Deldar, JHEP **0101**, 013 (2001)
8. L. Del Debbio, D. Diakono, Phys. Lett. B **544**, 202 (2002)
9. L. Del Debbio, M. Faber, J. Greensite, Nucl. Phys. B **414**, 594 (1994)
10. S. Ohta, M. Wingate, Nucl. Phys. **73** (Proc. Suppl.), 435 (1999); B. Lucini, M. Teper, Phys. Lett. B **501**, 128 (2001); L. Del Debbio, H.H. Panagopoulos, P. Rassi, E. Vicari, JHEP **0201**, 9 (2002)